ARTICLE

https://doi.org/10.1590/2317-4889202220220035

BJGEO
Brazilian Journal of Geology

Spectral characterization of the Umbuzeiro Doce skarn target (Brazil): insights for the exploration of a W-Mo-gemological vesuvianite system

Lília Albuquerque da Silva[1,2], Thais Andressa Carrino[2]*, Lauro Cézar Montefalco de Lira Santos[1,2], Rosa Elvira Correa Pabón[3]

Abstract

The Umbuzeiro Doce skarn target in the Seridó Belt (NE Brazil) was studied using reflectance spectroscopy and petrography. Interpretation of the 61 reflectance spectra obtained in the study established the following zones: marble zone, with diagnostic absorption features at 2,340 and 2,475 nm (C–O); tremolite marble zone, with main absorption at 1,393 (OH^-) and 2,313 nm (Mg–OH); garnet-vesuvianite zone, with the main absorption at 2,215 nm (OH^-); diopside-hornblende zone, marked by a broad absorption at 1,153 nm (Fe^{2+}); late wollastonite zone, which lacks a diagnostic spectral signature; and a local violet vesuvianite-bearing marble, characterized by potential gemological vesuvianite marked by Cr^{3+} absorption features (~548 and 680 nm). Centimeter-sized molybdenite aggregates occur at the interface of the marble and calc-silicate alteration zones. Spectral indices were produced to automate identification of potential zones to explore Mo, W, and gemological vesuvianite. Indices for the zones of marble, tremolite marble, garnet-vesuvianite, diopside-hornblende and violet vesuvianite were produced and tested. This methodology appears as a powerful exploratory guide for Mo, W, and violet vesuvianite occurrences or deposits that show a mineral zoning like the Umbuzeiro Doce target.

KEYWORDS: reflectance spectroscopy; spectral indices; hydrothermal alteration; violet vesuvianite; metal exploration.

INTRODUCTION

Spectral technologies appear as a powerful tool for exploration projects with already observed success mainly in metalliferous systems, such as VHMS, orogenic, SEDEX, and IOCG deposits (Tappert *et al.* 2011, Fresia *et al.* 2017, Lampinen *et al.* 2019, Naleto *et al.* 2019, Ross *et al.* 2019, Medina *et al.* 2021). The spectral technologies, such as reflectance and imaging spectroscopy, appear as advanced remote sensing data for detailed and rapid analysis of alteration minerals, including their distribution, and the definition of spectral indices as vectoring tools to locate proximal ore sites (Bedell *et al.* 2009).

The most abundant spectral case studies are based on instruments that detect electromagnetic radiation in the visible, near-infrared, and shortwave infrared range, equivalent to wavelengths from ~350 to 2,500 nm. The understanding of the spectral signature of a target is based on the physical principles related to electronic and molecular transitions (Hunt 1977, 1979, Clark *et al.* 1990, Clark 1999). The electronic transition is a process that affects metals such as Fe, Mn, Cr, and V. It is related to the most energetic ranges equivalent to the visible-near-infrared interval, with absorption features associated with the presence of some transition metal. In contrast, the molecular transition involves large wavelengths (lower energy), i.e., the shortwave infrared interval. In this case, absorption features are related to specific molecules, commonly hydroxyl (OH^-), water (H_2O), Al–OH, Mg–OH, Fe–OH, and carbonates (C–O) (Clark *et al.* 1990).

In metamorphic geological settings, metasomatic processes could form calc-silicate-rich alteration haloes common in skarn-related deposits. Their fertility involves large concentrations of metals such as Cu, Mo, W, Au, Sn, Pb, Ag, and REE (Meinert *et al.* 2005).

Spectral investigations were conducted worldwide concerning skarn deposits, mainly with reflectance spectroscopy. As expected, some spectral proxies or spectral indices were already proposed for different skarn environments, reflecting the mineralogical variability that hydrothermal processes could generate in different environmental conditions, such as host rock type, depth, metamorphic grade, and fluid/rock ratio (Meinert 1992, Meinert *et al.* 2005). For instance, the Ludwig Cu-bearing skarn, located in the Yerington District (Nevada, USA), was investigated using a portable spectroradiometer and hyperspectral images (Hymap) by Cudahy *et al.* (2001). These authors identified the spectral signature of alteration

[1]Programa de Pós-Graduação em Geociências, Universidade Federal de Pernambuco – Recife (PE), Brazil.
E-mails: lilia_albuquerque@hotmail.com, lauro.lsantos@ufpe.br

[2]Departamento de Geologia, Centro de Tecnologia e Geociências, Universidade Federal de Pernambuco – Recife (PE), Brazil.
E-mail: thais.carrino@gmail.com

[3]Instituto Tecnológico Vale – Ouro Preto (MG), Brazil.
E-mail: rosa.correa@itv.org

*Corresponding author.

minerals such as white mica, amphiboles, as well as calcite and dolomite that were used as spectral guides for exploration. Guo *et al.* (2019) characterized drill core samples from the Jiama Cu porphyry-skarn deposit (Tibet) using the HR-1024 spectroradiometer from the Spectra Vista Corporation. In this case study, the white mica compositional variation was established as an indicator for copper exploration. Thus, the 2,200 nm (Al–OH) wavelength position was selected as the spectral index, with the Cu-mineralized body presenting the Al–OH wavelength position between 2,203 and 2,206 nm. In addition, Guo *et al.* (2019) observed the rapid increase of Cu content when the Al–OH wavelength position is longer than 2,206 nm. Tian *et al.* (2019) studied the Cu–Au skarn deposit of Jiguanzui (China) using an ASD-TerraSpec in drill core samples, discriminating montmorillonite, illite, chlorite, muscovite, kaolinite, and carbonates. As a spectral index for targeting proximal ore sites, the authors observed the relation of abundant Al–OH-bearing silicates in the mineralized sectors with absorptions features centered at > 2,209 nm. Another proposed spectral index was based on the Fe–OH wavelength position at > 2,330 nm related to chlorites from the mineralized bodies.

In northeastern Brazil, specifically in the Seridó Belt, Costa *et al*. (2017) characterized hydrothermal minerals from the Brejuí W–Mo skarn deposit, such as phengitic illite, nontronite, chlorite, recrystallized calcite, and gypsum using an ASD-FieldSpec. In addition, the authors mapped carbonate- and smectite-rich targets related to the mineralized areas using the ProSpecTIR-VS hyperspectral images. Recently, Mesquita *et al*. (2019), using an ASD-FieldSpec, detailed the main active minerals from a drill core of the Bonfim W–Mo–Au skarn deposit, also in the Seridó Belt. Specifically for Au exploration, a spectral guide based on the prehnite abundance, coeval to Au mineralization, was created. Thus, the prehnite spectral index was proposed using the diagnostic absorption centered at 1,478 nm (OH^-).

The previous studies in skarn deposits from the Seridó Belt highlight the potential use of reflectance spectroscopy to aid rapid mineral zoning discrimination, vectoring the metal exploration sites. Concerning this W–Mo exploration region from NE Brazil, new case studies using reflectance spectroscopy can be performed systematically to characterize other skarn deposits and targets. Thus, the goal of this research is to target hydrothermal alteration zones to explore Mo and/or W, and the unusual occurrence of gemological violet vesuvianites in the Umbuzeiro Doce target, by creating a pioneer spectral indices-driven approach.

GEOLOGICAL SETTING

Being located in the South American Platform, the Borborema Province is a Neoproterozoic orogen with Archean and Paleoproterozoic blocks metamorphized and deformed at *ca.* 600–500 Ma, and abundant Ediacaran-Cambrian plutons related to the Western Gondwana collage during the Neoproterozoic (Almeida *et al.* 1981, Hollanda *et al.* 2010, Brito Neves *et al.* 2014, Caxito *et al.* 2020, Santos and Caxito 2021). This province is commonly divided into three sub-provinces (Northern, Central, and Southern), all of them being segmented by extensive E-W and NE-SW shear zones (Van Schmus *et al.* 1995, 2003) (Fig. 1A).

According to Brito Neves *et al.* (2000), three geotectonic domains characterize the Northern Subprovince of the Borborema Province: Médio Coreaú, Ceará Central, and Rio Grande do Norte. The main W-, W–Mo-, and Au-bearing skarns occur in the Rio Grande do Norte Domain, which is limited by the Senador Pompeu Shear zone in the west, the Potiguar Basin in the north, and Patos Shear Zone in the south (Figs. 1A and 1B). The Rio Grande do Norte Domain groups the Orós-Jaguaribe Belt (Paleoproterozoic gneiss-migmatite basement, granite, and volcano-sedimentary rocks), the Rio Piranhas Terrain (Early to late Paleoproterozoic gneiss-migmatite basement), the Seridó Belt (Late Neoproterozoic meta-supracrustal rocks), the Granjeiro Terrain (High-grade Archean metamorphic rocks), and the *ca.* 3.5 Ga São José do Campreste Massif (Archean gneisses and plutono-volcanic intrusions) (Dantas *et al*. 2004, Velásquez Ruiz *et al.* 2019, Santos *et al.* 2020, among others).

The main polymetallic deposits (e.g., Bodó, Brejuí, and Bonfim) and other skarn targets are found in the metapelite and metapsamite rocks of the Seridó Group (part of the Seridó Belt), aged between 650 and 610 Ma (Van Schmus *et al.* 2003, Hollanda *et al.* 2017) that overlain *ca.* 2.2–2.1 Ga basement (gneisses and migmatites). This set was also intruded by several Ediacaran-Cambrian magmatic suites and crosscut by a complex network of NNE-SSW shear zones (Nascimento *et al.* 2015).

The Seridó Group is composed of the Serra dos Quintos Formation (metavolcanosedimentary rocks) at the base, followed by the Jucurutu (metapelites and carbonate rocks), Equador (quartzite and meta-conglomerate), and Seridó (micaschist) formations (Santos *et al.* 2014 and references therein). Many skarn targets and some deposits bearing W, W–Mo, and W–Mo–Au–Te–Bi occur associated with marbles from the Jucurutu Formation or in contacts between micaschists (Seridó Formation) and marbles/paragneiss (Souza Neto *et al.* 2008, Santos *et al.* 2014). The main fertile region is called Seridó Tungsten Province (Fig. 1B). The genesis of polymetallic skarns is associated with low- to high-grade metamorphic events with a peak at *ca.* 575 Ma (Archanjo *et al.* 2013, Nascimento *et al.* 2015, Souza *et al.* 2016), related to extensive shear zones, and the emplacement of numerous granites aged at the 600–593, 575–560, 548–533, 528–510, and 495–450 Ma intervals (Souza *et al.* 2016). These intrusions comprise gabbros, diorites, porphyritic monzogranites, alkali to peralkaline granites, and syenogranites (Archanjo *et al.* 2013, Nascimento *et al.* 2015, Souza *et al.* 2016).

Mineralized skarns at the Seridó Belt were generated by metasomatic processes coeval with the emplacement of igneous intrusions and regional metamorphic events, mainly at *ca.* 600–525 Ma (Hollanda *et al.* 2017). For instance, scheelite comprises the main ore mineral, followed by molybdenite, while gold is associated with late mineralization, at least in the Bonfim Deposit (Souza Neto *et al.* 2008), corroborating the strong metallogenetic potential of the region.

The study target comprises the Umbuzeiro Doce skarn, which is located in the Santa Luzia municipality (UTM

zone 24 south, 0738494 W; 9235114 S), Paraíba State, NE Brazil (Fig. 1B). In this target, previous studies characterized skarn pockets as centimeter- to metric-sized (~2–3 m), in contact with Jucurutu Formation marbles or Seridó Formation schists (Ferreira *et al.* 2014, Paixão *et al.* 2019). The skarns are mainly characterized by scheelite, molybdenite, and violet vesuvianite crystals, which were previously identified with gemological potential by Ferreira *et al.* (2014). According to Paixão *et al.* (2019), the region is marked by marble composed of calcite, interstitial graphite, scarce chalcopyrite, and pyrite. The metasomatic alteration zones are composed of diopside-, hornblende-, dark brown vesuvianite-, and garnet-rich zones. A late halo surrounds the other alteration zones and is composed mainly of radial wollastonite and calcite. Unusual violet vesuvianites were observed in scarce outcrops of the Jucurutu Formation marble, as coarse-grained violet crystals. The violet color is derived from Cr^{3+} absorption bands (~575 and 690 nm) determined by UV-Vis spectroscopy (Ferreira *et al.* 2014).

METHODOLOGY

A total of 28 fresh rock samples from the Umbuzeiro Doce target were collected, including Jucurutu Formation marbles and hydrothermal alteration zones.

Thin polished sections (n = 16) were produced for the mineralogical and textural analysis of the samples. In addition, millimetric violet vesuvianite crystals were analyzed and photographed using a Schneider gemological microscope coupled with a Canon EOS 1100D digital camera from the Laboratory of Gemology of Universidade Federal de Pernambuco, Brazil.

The samples were submitted to spectral reflectance measurements in the Vale Institute of Technology (Brazil) using the ASD-FieldSpec®4-High-Resolution Next Generation. This instrument is marked by 2,151 channels in the visible to shortwave infrared range (Malvern Panalytical 2022). The calibration was done using a Lambertian plate (Spectralon®), and 2-6 reflectance measurements were done per sample. For qualitative interpretation of active minerals in the spectral curves, each spectrum was investigated in reflectance and

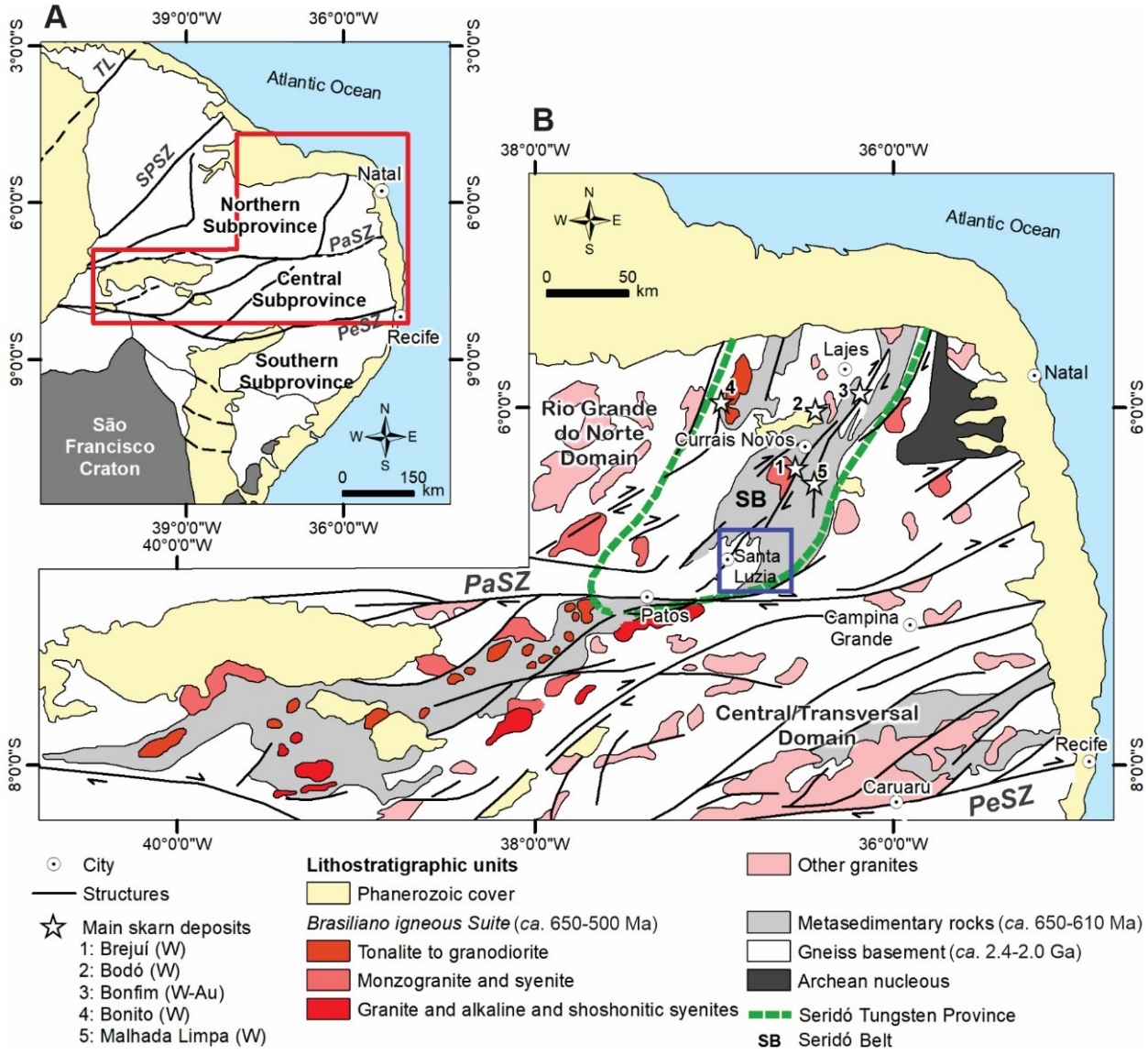

Source: (A) modified from Van Schmus *et al.* (2008); (B) modified from Souza Neto *et al.* (2008) and Mesquita *et al.* (2019).
SPSZ: Senador Pompeu Shear Zone; PaSZ: Patos Shear Zone; PeSZ: Pernambuco Shear Zone; TL: Transbrasiliano Lineament.

Figure 1. (A) Main geotectonic division of the Borborema Province. (B) Simplified geological map of the Seridó Belt region, located in the Rio Grande do Norte Domain. The blue rectangle demarks the region of Santa Luzia municipality where the Umbuzeiro Doce skarn target is located.

normalized reflectance using the continuum removed technique (hull quotient) explained by Clark and Roush (1984). The Hyperspectral Python software (HypPy; Hecker *et al.* 2019) was used for this step. After the spectral-mineralogical interpretation, all normalized reflectance spectra (ASCII format) were organized in a single file using the licensed Excel (Microsoft Office®) software. In this step, spectra arithmetic was tested, and the spectral indices were established for the recognition of lithotypes and hydrothermal alteration zones, exploring the spectral gradients that demark typical active minerals from each target. For a better understanding of the spectral indices' performance, scatterplots were generated to visualize the separation of different rocks/alteration zones. For this purpose, the Orange Data Mining (v. 3.32) software was selected.

RESULTS AND DISCUSSION

Petrography and spectral characterization

The Umbuzeiro Doce target is characterized by distal zones (e.g., marble and tremolite marble) toward the proximal centimeter- to metric-sized garnet-vesuvianite and diopside-hornblende alteration zones, which are the main potential sites for W and Mo exploration. The occurrence of violet gemological vesuvianite was also recognized in a local marble site. This study focused on three skarn pockets marked by ~2–3 m width (Fig. 2), with no clear evidence of faulting or shearing.

Marble

Jucurutu Formation marbles are mainly characterized by calcite (*ca.* ~95% modal composition) and mafic banding (Fig. 3A). In thin sections, the marble is characterized by xenoblastic to hypidioblastic calcite and characteristic tabular thick twins. The calcite defines the granoblastic texture. The apatite and zircon are inclusions (Fig. 3B) and disseminated intergranular sulfides (e.g., pyrite, chalcopyrite) also occur like hydrothermal phases (Fig. 3C).

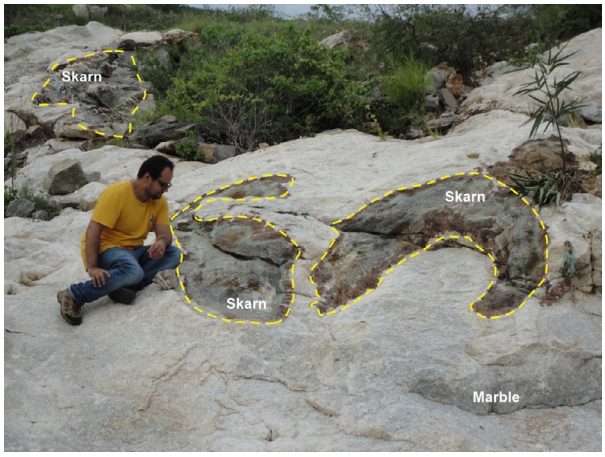

Figure 2. Overview of the Umbuzeiro Doce target, marked by marbles from the Jucurutu Formation, and skarn rocks.

The spectral reflectance signature is dominated by a broad absorption feature of ferrous iron (biotite or phlogopite) in the visible to the near-infrared range. Calcite absorption features are centered at 1,754, 1,786, 1,962, 2,160, 2,292, 2,340, and 2,475 nm (arising from C–O vibrational processes), and subtle features at 1,400 nm (OH^-) and 2,400 nm (Mg–OH) may represent minor contents of biotite/phlogopite (Hunt 1977, Gaffey 1986; Fig. 3D).

Tremolite marble

Tremolite marble is mainly characterized by calcite (*ca.* 75% modal composition), acicular-like tremolite, and disseminated pyrite (Figs. 4A and 4B).

Under the microscope, recrystallized calcite is hypidiomorphic and shows quartz inclusions in some crystals. The amphibole forms acicular aggregates, defining a nematoblastic texture (Fig. 4B). Tremolite crystals are of ~200–> 2,000 µm size and indicate greenschist to amphibolite facies, being the main index mineral of this marble (Fig. 4C). Observing the reflectance spectra, the tremolite absorption features predominate and are centered at 1,024 nm (ferrous iron), 1,393 (OH^-), 2,250 nm (Fe–OH), 2,300, 2,313, and 2,386 nm (Mg–OH) (Hunt 1977, Pontual *et al.* 2008).

Garnet-vesuvianite alteration zone

Centimeter-sized dark brown vesuvianite and garnet crystals are the main alteration minerals of this zone, marked by reddish color (Fig. 5A). The garnet megacrysts could show intense fracturing and calcite or vesuvianite inclusions. Diopside crystals may appear as disseminated inclusions in the garnet and vesuvianite megacrysts, defining a poikiloblastic texture (Fig. 5B). Centimeter-sized molybdenite aggregates are observed in this alteration zone at the interface with the marble (Fig. 5C).

The spectral characterization of this calc-silicate zone is occasionally marked by absorption features arising from weathering, with the goethite detected by ferric iron absorptions at ~428, 686, and 905 nm (Hunt 1977; Fig. 5D). However, the dark brown vesuvianite absorption features are dominant. This mineral has a chemical formula of $X_{19}Y_{13}Z_{18}T_{0\text{-}5}O_{68}W_{10}$, where X = Ca^{2+}, Na^+, Ln, Pb^{2+}, Sb^{3+}; Y = Al^{3+}, Mg^{2+}, Fe^{2+}, Ti^{2+}, Mn^{2+}, Cu^{2+}, Zn^{2+}, Cr^{3+}; Z = Si^{4+}; T = B^{3+}; and W = (O^{2-}, OH^-, F^-) (Groat and Hawthorne 1998). The vesuvianite absorption features are centered at 901 and 1,165 (ferrous iron), 1,405 (OH^-), 1,436 (OH^-), 1,482 (OH^-), 1,836 (OH^-), and 1,921 and 1,962 nm (probably water and/or OH^-) (Groat *et al.* 1995). The main absorptions are in 2,047, 2,215, 2,306, 2,363, 2,385, and 2,436 nm (Fig. 5D) and could represent the OH^- stretching process. The absorption features in the 1,400 nm range indicate the F-bearing vesuvianites, according to the mineral chemistry and spectroscopy studies by Groat *et al.* (1995).

Diopside-hornblende alteration zone

This alteration zone occurs in the central portion of the skarns. It is greenish, representing high amphibole and pyroxene content (Fig. 6A). A granoblastic texture is observed in thin sections, with xenomorphic to hypidiomorphic quartz and plagioclase, xenoblastic to hypidioblastic calcite, and xenoblastic

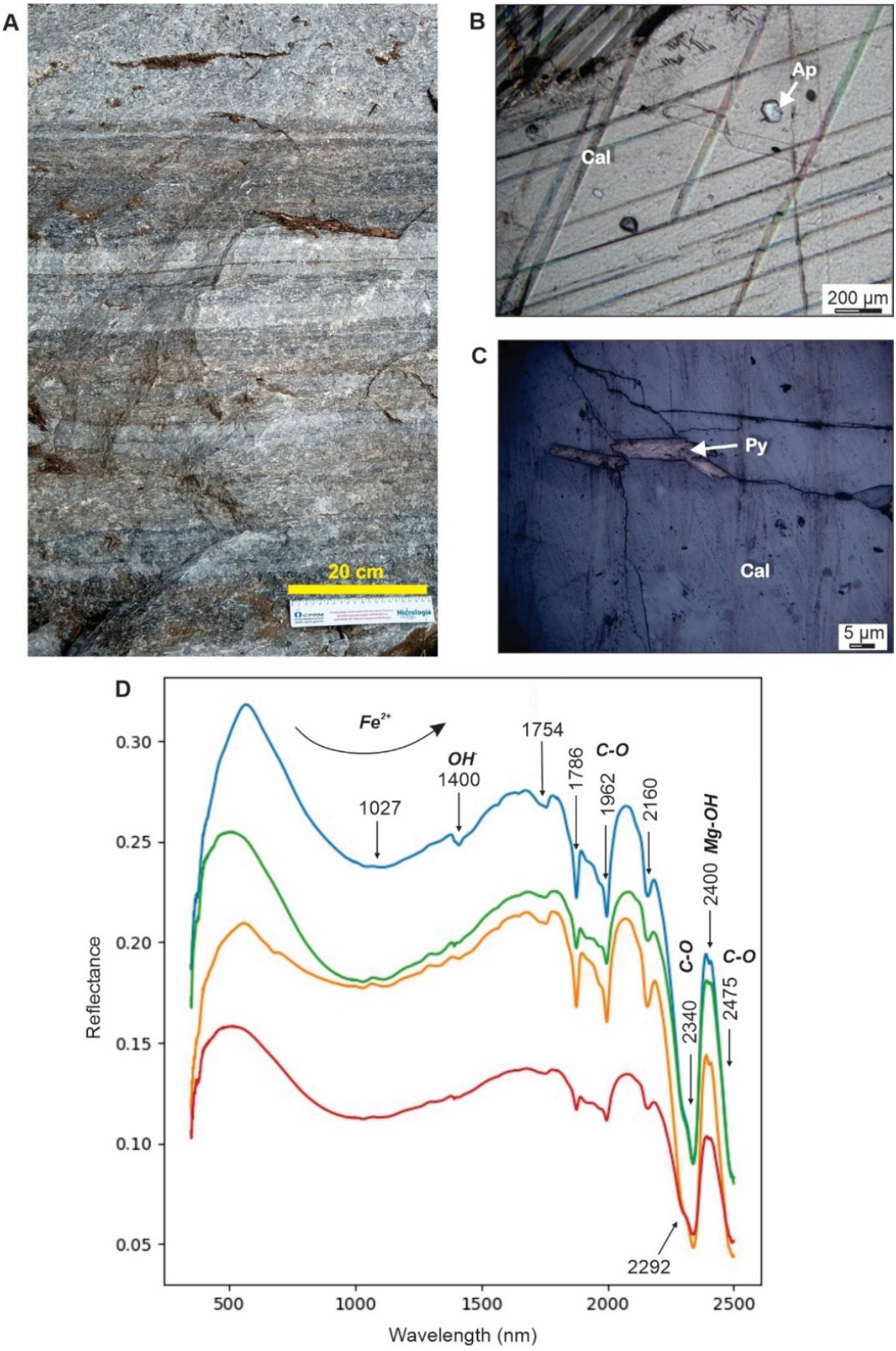

Ap: apatite; Cal: calcite; Py: pyrite.

Figure 3. (A) Example of banded marble outcrop, and (B) mineral phases observed under a transmitted plane-polarized light and (C) reflected plane-polarized light microscope. (D) Four reflectance spectra of Jucurutu Formation marbles show C–O absorption features of calcite and subtle iron, OH^-, and Mg–OH absorptions from biotite or phlogopite.

diopside and hornblende (Figs. 6B and 6C). The main opaque minerals are pyrite and chalcopyrite, which appear disseminated throughout the rock.

The spectral reflectance signature shows a broad absorption feature of ferrous iron in the visible to the near-infrared interval, associated with both pyroxene and amphibole (Fig. 6D). Absorptions at ~1,400 (water and/or OH^-) and 1,900 nm (water) also occur and could be deeper when hydrated minerals are abundant. Subtle absorption features at ~2,200 nm could represent a weathering clay mineral, for example, and the subtle absorption at ~2,320 nm (Mg–OH) could be associated with hornblende. Prehnite [$Ca_2Al_2Si_3O_{10}(OH)_2$] is scarcely observed by diagnostic absorption features at 1,477, 2,233, 2,288, and 2,354 nm, derived from OH^- vibrational process (Pontual *et al.* 2008, White *et al.* 2017).

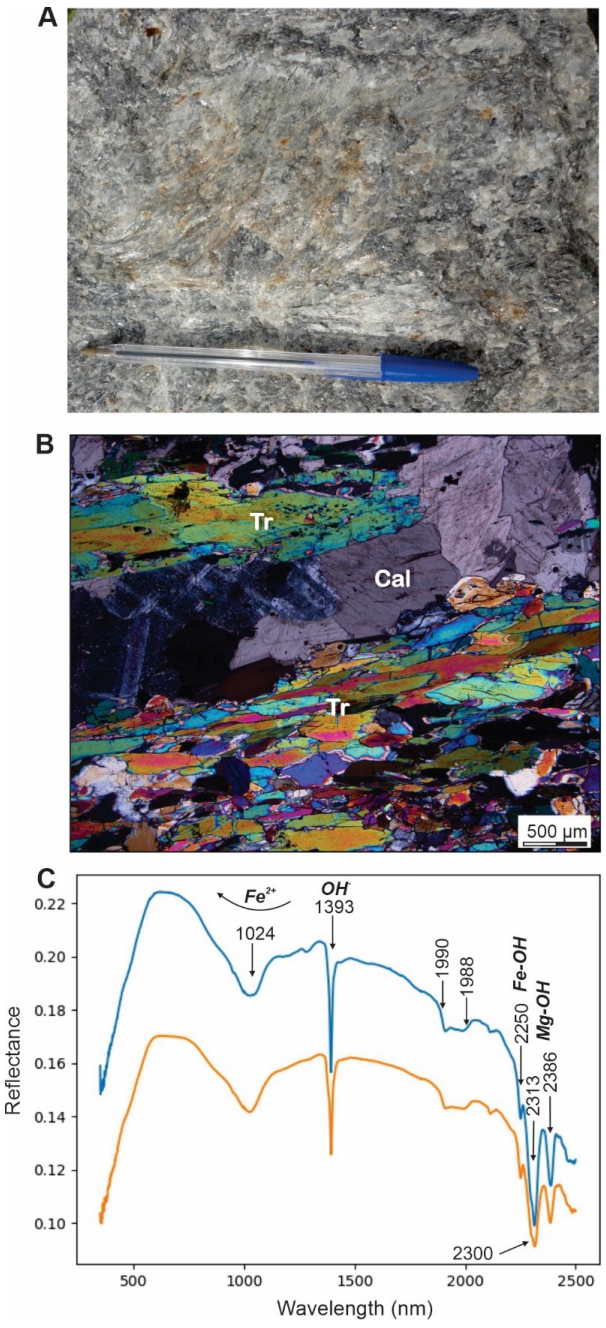

Cal: calcite; Tr: tremolite.

Figure 4. (A) Acicular tremolite aggregates in calcite marbles, (B) also observed under crossed nicols, showing nematoblastic texture. (C) Two reflectance spectra of tremolite marble showing absorption features of ferrous iron, OH^-, Fe–OH, and Mg–OH.

Wollastonite-rich alteration zone

The wollastonite-rich alteration zone is marked by whitish color and fibrous and radial wollastonite (Fig. 7A), up to 5 cm in size. This alteration zone envelops other zonings such as the garnet-vesuvianite and diopside-hornblende. Also, it appears as a late hydrothermal alteration, filling ~E-W fractures that cut calc-silicate alteration zones (Figs. 5A and 6A).

The wollastonite ($CaSiO_3$) is a nonactive mineral in the visible to shortwave infrared range (Cloutis 2002), and the spectral reflectance signature of this zone is marked by absorption features of dark greenish-brown vesuvianites that occur as scarce crystals (Figs. 7A and 7B). Thus, reflectance spectroscopy does not work well to separate this alteration zone in relation to others characterized by vesuvianite (e.g., garnet-vesuvianite zone and violet vesuvianite-rich zone).

Local violet vesuvianite-bearing marble

A local outcrop of coarse-grained violet vesuvianite crystals was found in the Jucurutu Formation marbles (Fig. 8A), associated with alteration minerals such as acicular tremolite, hornblende, and calcite. Some vesuvianites have calcite inclusions (Fig. 8B) and their color is explained by the absorption features at ~548 and 680 nm arising from Cr^{3+} (Fig. 8C). These absorptions are unique to differentiate the vesuvianite composition varieties. In contrast, other absorption features centered at ~900, ~1,000, ~1,400, ~1,434, 1,482-1,486, ~1,837, ~1,920, ~1,970, ~2,050, 2,215, 2,305, ~2,370, and ~2,435 nm are similar to both dark brown and violet vesuvianite (Figs. 5D and 8D).

Spectral indices to target exploratory sites

Spectral indices are established by recognizing spectral gradients, i.e., the contrast of high and low reflectance in specific wavelength positions that demark a certain mineral to target. This procedure is observed in case studies of different deposits or prospects in the literature, such as Tappert *et al.* (2011), Yang *et al.* (2011), Prado *et al.* (2016), Mesquita *et al.* (2019), and Medina *et al.* (2021), mainly for estimating the mineral abundance of specific mineral groups based on the depth of diagnostic absorption features or using spectral arithmetic. In this research, we analyzed the spectral responses of each lithotype and alteration zone (Fig. 9) and determined the main diagnostic absorption feature to separate each one. Our analyses consider only the fresh rock spectral responses to create spectral indices toward automatized applications, for example, rapid spectral mineral discrimination in well-preserved outcrops or systematic analysis of drill cores. We do not assume a weathering exploratory context.

The first step was to select the potential spectral ranges focusing on rapid mineralogical discrimination that could be useful to distinguish carbonate-, calc-silicate-, and violet vesuvianite-rich targets. The second step involved the creation of spectral indices based on normalized reflectance spectra (continuum removed technique; Clark and Roush 1984), as shown in Table 1, and the interpretation of the indices' performance in 61 reflectance measurements (Figs. 10 and 11).

Based on the above considerations, the proposed indices were produced using spectra ratios driven by the following diagnostic spectral gradients:

- For the marble: The main absorption feature of calcite, not ambiguous to the most common minerals in the study area, is that centered at 2,475 nm (Fig. 9). Only tremolite shows a similar absorption feature at ~2475 nm, but it shows a low intensity in relation to calcite. Thus, the marble index (MI) is based on the ratio of reflectance data centered at 2,414 nm (high reflectance values for calcite) and 2,475 nm (low reflectance values). This index works well for discriminating marble with a cutoff value ≥ 1.10 (Fig. 10A);
- For the tremolite marble: The unambiguous absorption feature of tremolite is centered at 1,393 nm (OH^-) (Fig. 9). The tremolite marble spectral index (TMI) is marked by a ratio of reflectance values at 1,360 nm (numerator) and 1,393 nm (denominator). In this case, the TMI works successfully with a cutoff value ≥ 1.10 (Fig. 10B);
- For the garnet-vesuvianite alteration zone: The spectral index of the garnet-vesuvianite zone (GVI) was created based on the dominant dark brown vesuvianite spectral signature. Thus, the diagnostic absorption feature centered at 2,215 nm (OH^-) was explored, by the determination of the reflectance ratio at 2,140 nm (numerator) and 2,215 nm (denominator). This approach implies GVI value ≥

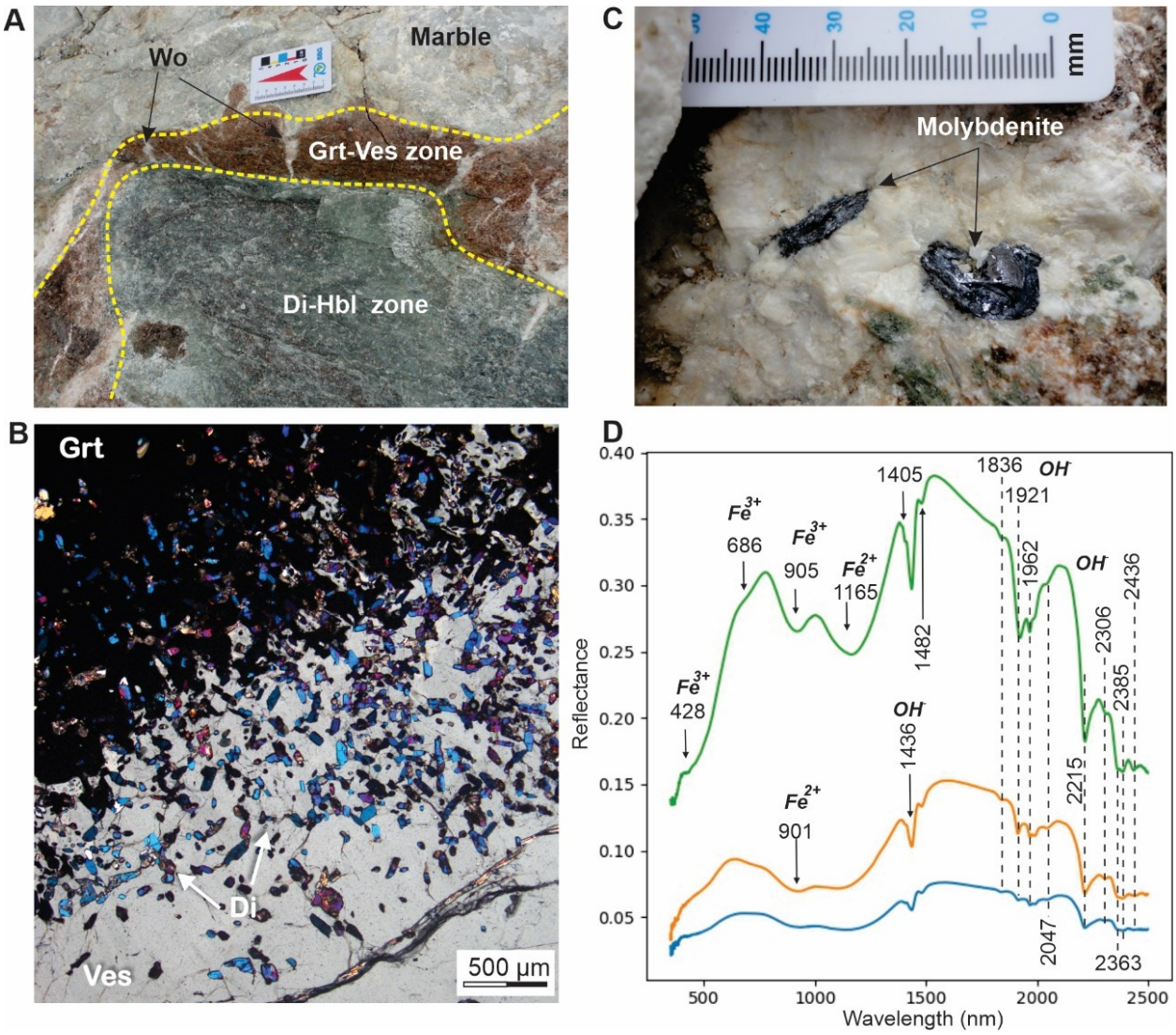

Di: diopside; Grt: garnet; Hbl: hornblende; Ves: vesuvianite; Wo: wollastonite.

Figure 5. (A) Detail of garnet-vesuvianite alteration zone outcrop. (B) Photomicrography of garnet and vesuvianite both poikiloblastic with diopside inclusions, under crossed nicols. (C) Detail of centimeter-sized molybdenite aggregates. (D) Typical reflectance spectra are dominated by dark brown vesuvianite absorption features, related to ferrous iron and OH^-.

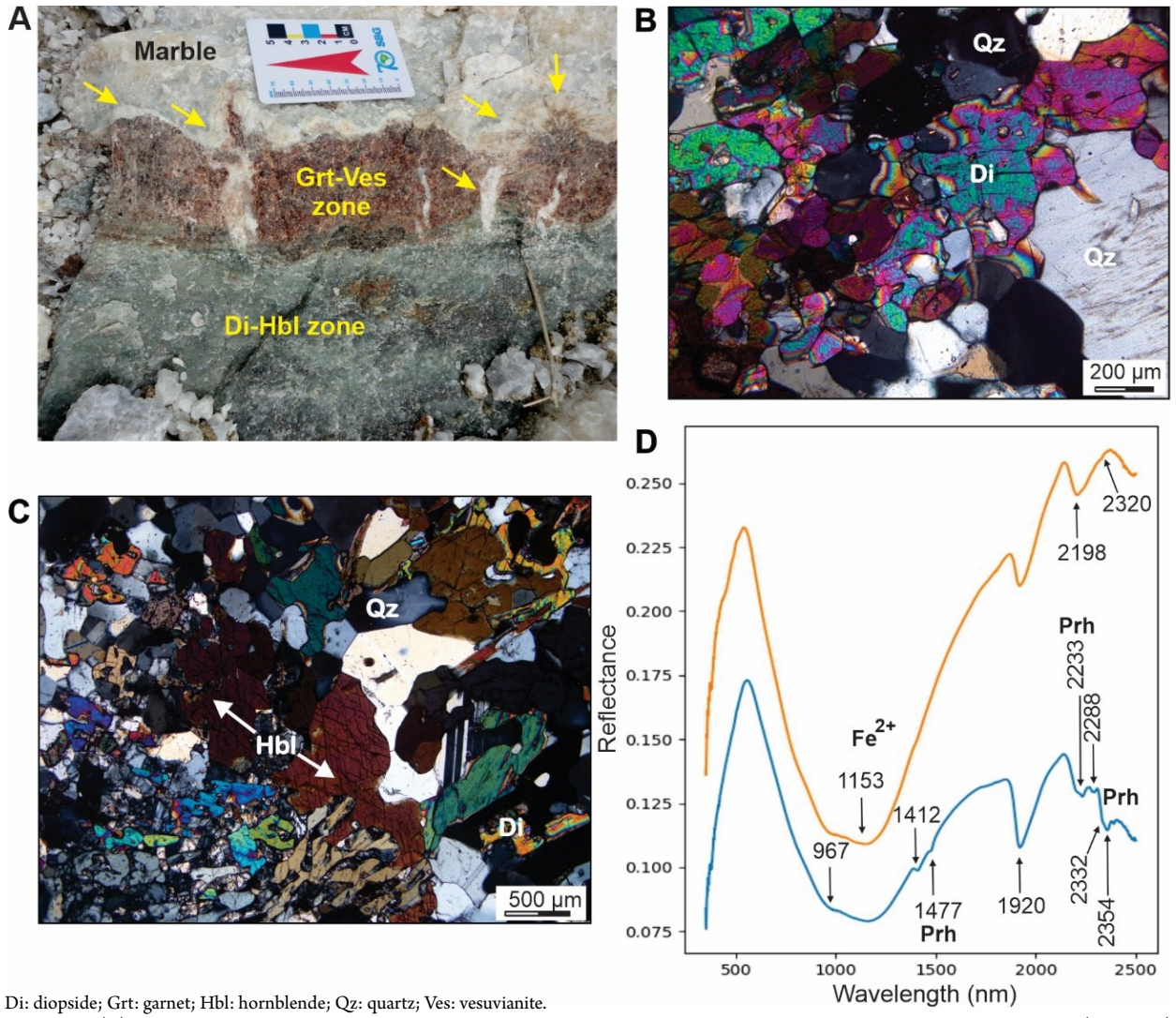

Di: diopside; Grt: garnet; Hbl: hornblende; Qz: quartz; Ves: vesuvianite.

Figure 6. (A) Example of diopside-hornblende alteration zone outcrop; arrows indicate wollastonite-rich alteration zone. (B and C) Photomicrographs (crossed nicols) display the main minerals from the diopside-hornblende zone. (D) Reflectance spectra are dominated by broad iron absorption features from amphibole and pyroxene and absorptions of prehnite (Prh) in some samples.

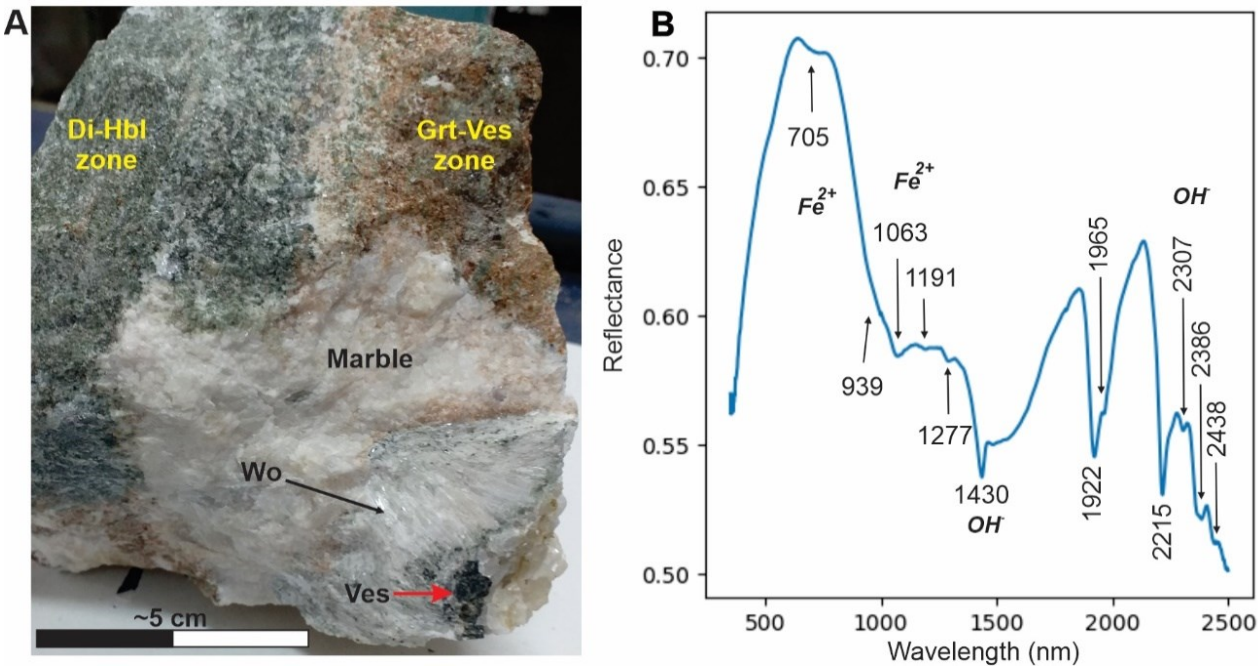

Di: diopside; Grt: garnet; Hbl: hornblende; Ves: vesuvianite; Wo: wollastonite.

Figure 7. Wollastonite-rich alteration zone characterized by (A) centimeter-sized fiber-like wollastonite aggregates and (B) its spectral signature. As a nonactive mineral, wollastonite does not show spectral features, prevailing the absorptions of scarce dark greenish brown vesuvianites.

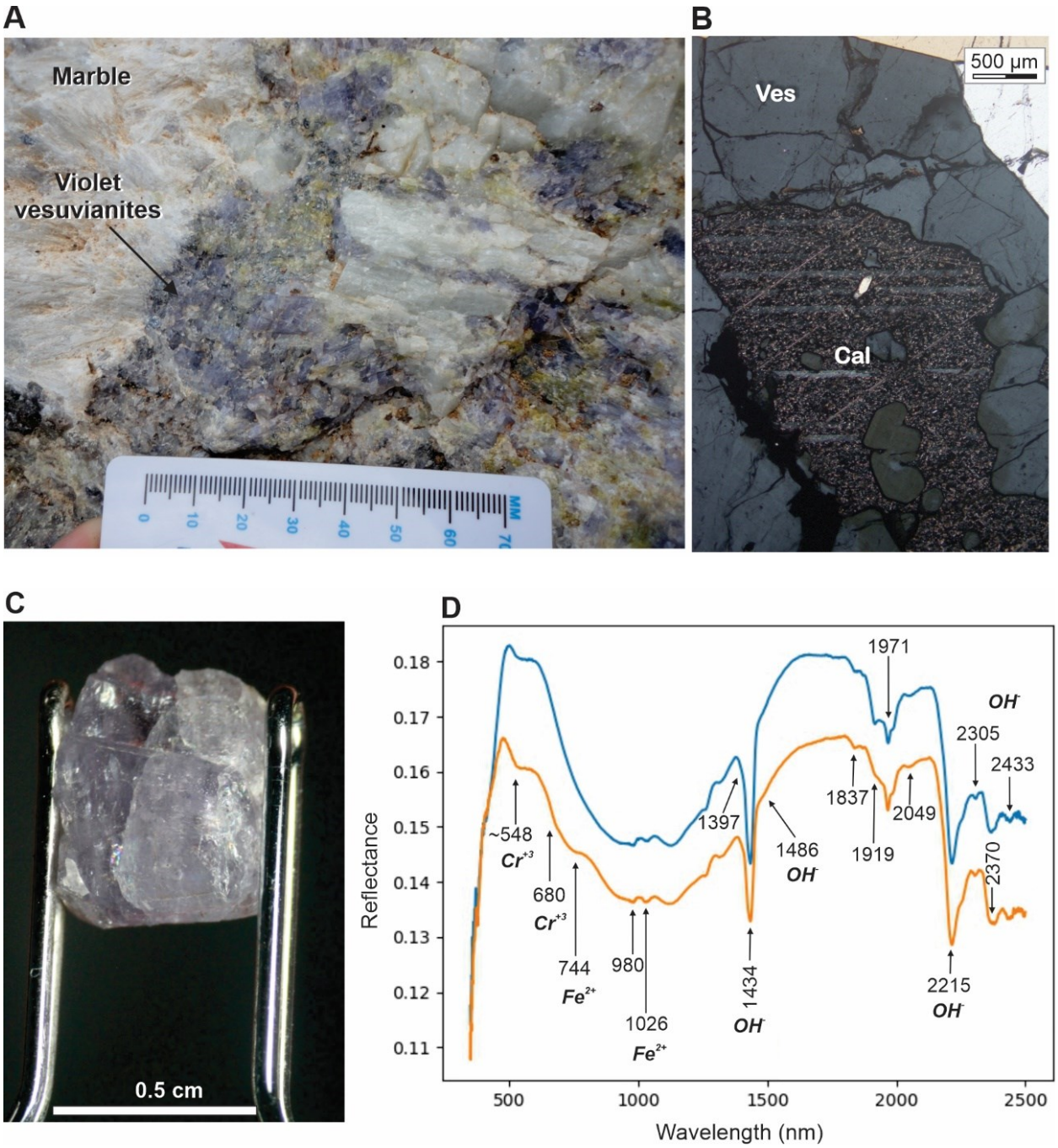

Figure 8. (A) Local occurrence of violet vesuvianite-bearing marble, and (B) photomicrography, under crossed nicols, showing growth of vesuvianite associated with calcite. (C) Violet vesuvianite crystal observed under a gemological microscope, and (D) reflectance spectra marked by Cr^{3+} absorption features that appear as a reliable guide for violet vesuvianite exploration.

1.10 as a reliable cutoff value for discriminating dark brown vesuvianite-bearing samples (Fig. 10C). However, special attention should be given to the Umbuzeiro Doce target: high GVI values are also observed in samples from the wollastonite-rich zone because the wollastonite is a non-active mineral in the visible to shortwave infrared range, and scarce dark greenish-brown vesuvianites appear in the spectral response. Thus, the wollastonite-rich alteration zone is not easily discriminated with the spectral indices proposed in this work;

- For the diopside-hornblende alteration zone: The broad ferrous iron absorption feature in the visible to near-infrared was chosen for developing the spectral index of the diopside-hornblende zone (DHI). Even with the broad absorption features related to iron-bearing minerals (e.g., vesuvianite and mafic minerals in banded marble; Fig. 9), the index was created based on more complex arithmetic that explores high reflectance peak (500 nm) and deep absorption features (1,153 and 1,380 nm) that could separate the diopside-hornblende

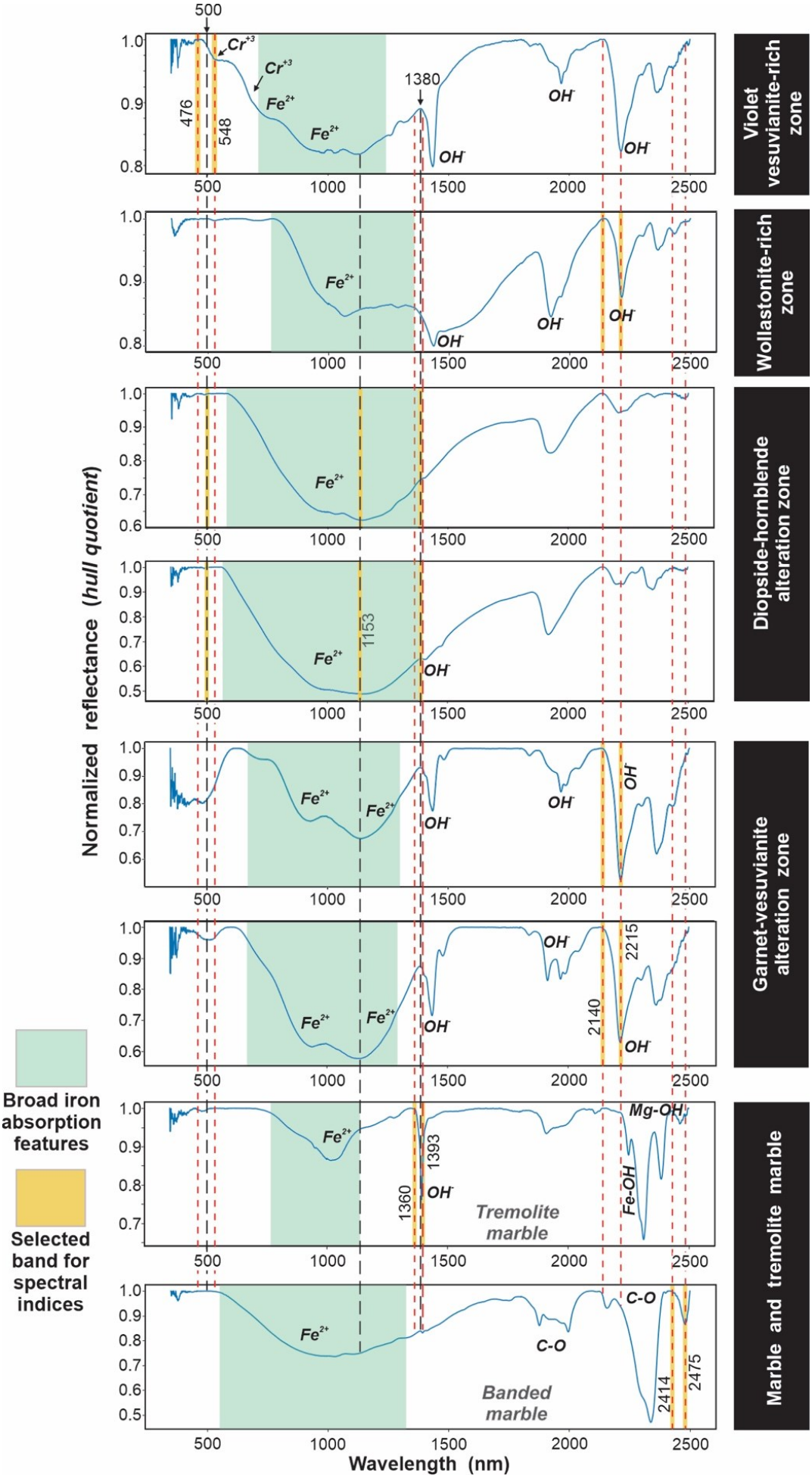

Figure 9. Comparison of normalized reflectance spectra of the marble, tremolite marble and mineral zones from the Umbuzeiro Doce skarn target to interpret diagnostic spectral gradients for differentiating each zoning.

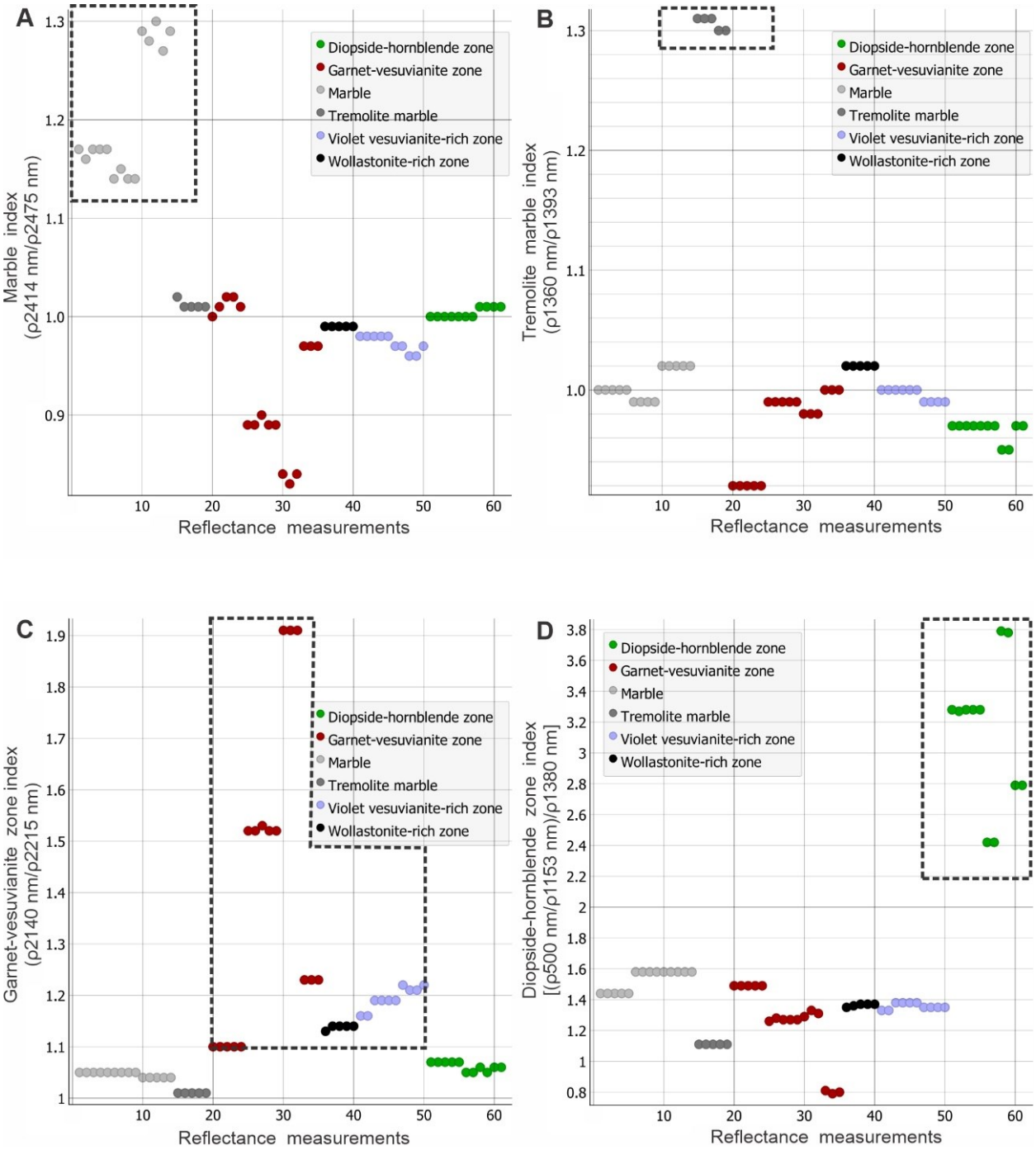

Figure 10. (A) Scatterplots of spectral index of marble, (B) tremolite marble, (C) garnet-vesuvianite zone, and (D) diopside-hornblende zone for 61 reflectance measurements. Note the reliable discrimination of each lithotype/alteration zones (black dotted outline polygons) using the proposed spectral indices.

alteration zone from others. The DHI [(reflectance at 500 nm/reflectance at 1,153 nm)/reflectance at 1,380 nm] values ≥ 2.20 work well for differentiating this zone from others in the studied region (Fig. 10D);

- For the violet vesuvianite-rich marble: Based on the violet vesuvianite-bearing spectra, the diagnostic and unique Cr^{3+} absorption feature centered at 548 nm was chosen to produce the violet vesuvianite spectral index, or VVI (Fig. 9, Table 1). Thus, we explored the spectral gradient of high reflectance at 476 nm and the low reflectance at 548 nm. VVI > 1 is an indicator for selecting violet vesuvianite-rich samples in the Umbuzeiro Doce region (Fig. 11A). In addition, the combined analysis of the GVI and VVI data permits better discrimination of the dark brown and violet vesuvianite varieties, a crucial step for defining different exploratory sites, i.e., potential samples or sites bearing metal (W, Mo) and gemological vesuvianites (Fig. 11B).

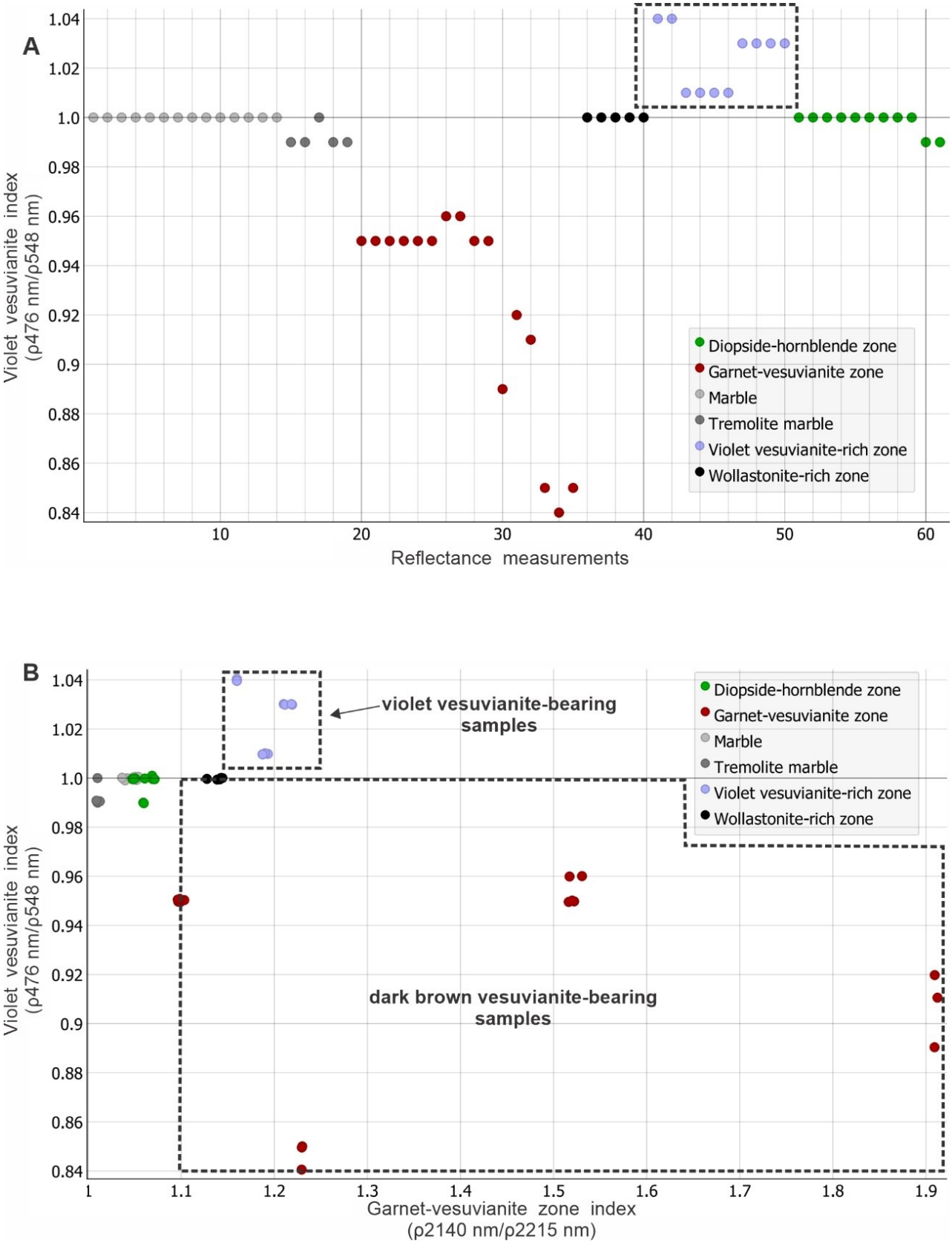

Figure 11. (A) Scatterplot of violet vesuvianite index for 61 reflectance measurements showing efficient discrimination of the violet variety of this silicate (black dotted outline polygon). (B) The comparison of the garnet-vesuvianite and the violet vesuvianite spectral indices shows better discrimination of the dark brown vesuvianite- and violet vesuvianite-rich samples using the combined approach of spectral indices.

Table 1. Summary of active minerals in the visible to shortwave infrared range using an ASD-FieldSpec and potential spectral indices proposed in this research.

Lithotype or mineral zones	Main active mineral(s) in the visible to shortwave infrared range	Main diagnostic absorption features	Proposed spectral indices to highlight mineral zones**	Main economic potential verified in this research and previous works[1,2]
Distal: marble	Recrystallized calcite, mafic minerals (biotite or phlogopite)	Calcite: 2,340 and **2,475 nm*** (C-O)	Criteria: abundant calcite. Spectral index: MI or marble index (ρ2,414 nm/ρ2,475 nm)	-
Distal: tremolite marble	Tremolite	Tremolite: 1,024 nm (ferrous iron), **1,393 nm*** (OH^-), ~2,300 nm (Mg-OH)	Criteria: abundant tremolite. Spectral index: TMI or tremolite marble index (ρ1,360 nm/ ρ1,393 nm)	-
Proximal: garnet-vesuvianite alteration zone	Dark brown vesuvianite	Vesuvianite: ~900, 1,165 nm (ferrous iron), ~1,400, ~1,836, ~1,962, ~2,047, **2,215***, ~2,306, ~2,385 nm (OH^-)	Criteria: abundant dark brown vesuvianite. Spectral index: GVI or garnet-vesuvianite zone index (ρ2,140 nm/ ρ2,215 nm)	
Proximal: diopside-hornblende alteration zone	Amphibole and pyroxene. Locally, prehnite	Amphibole and pyroxene (e.g., hornblende, diopside): broad ferrous iron absorption feature centered at **~1,153 nm***	Criteria: abundant amphibole and pyroxene. Spectral index: DHI or diopside-hornblende zone index [(ρ500 nm/ ρ1,153 nm)/ρ1,380 nm]	Molybdenite and scheelite occur in these three calc-silicate alteration zones or the interface with marble
Proximal: wollastonite-rich alteration zone	Scarce dark vesuvianite, in the interface with other alteration zones or marble	Subtle absorption features of dark greenish brown vesuvianites are predominant in the wollastonite-rich alteration zone. Wollastonite does not show absorption features	-	
Proximal: violet vesuvianite-rich alteration zone	Violet vesuvianite	Violet vesuvianite: same absorption features described in the garnet-vesuvianite-bearing samples. The absorption features at **548* and 680* nm** (Cr^{3+}) are diagnostic of the violet vesuvianite variety	Criteria: abundant coarse-grained crystals of violet vesuvianite. Spectral index: VVI or violet vesuvianite index (ρ476 nm/ρ548 nm)	Violet vesuvianite (for gemological exploration)

[1]Ferreira *et al.* (2014); [2]Paixão *et al.* (2019); *wavelength position of diagnostic absorption features that persists in some conditions of mineral mixtures, considering fresh rocks. These absorption features were used to produce spectral indices; **spectral indices rounded to two decimal places.

CONCLUSIONS

The Umbuzeiro Doce target shows a mineral assemblage mainly composed of calcite, tremolite, garnet, dark brown vesuvianite, diopside, hornblende, wollastonite, molybdenite, pyrite, and violet vesuvianite. A typical prograde metamorphic assemblage is mainly characterized by garnet, hornblende, diopside, and wollastonite, while hydrated minerals, such as amphiboles (e.g., tremolite) and vesuvianite, could represent the retrograde metamorphic phase, commonly observed in supracrustal-dominated domains (Meinert 1992, Meinert *et al.* 2005), including the Seridó Belt (*cf.* Souza Neto *et al.* 2008, Mesquita *et al.* 2019).

The use of reflectance spectroscopy permitted the creation of an initial spectral library of the Umbuzeiro Doce skarn. Reflectance spectra of marble, tremolite marble, diopside-hornblende-, and garnet-vesuvianite-rich alteration zones were discriminated against, including scarce violet vesuvianite-bearing rock samples.

The visual analysis of reflectance spectra allowed the determination and selection of the standard signatures for each lithotype/alteration zone as the first step for producing spectral indices to optimize rapid discrimination of hydrothermal zoning in skarns like Umbuzeiro Doce target. As powerful vectoring tools, the proposed spectral indices can highlight the distal alteration zones (marble and tremolite marble), proximal zones for Mo and/or W (diopside-hornblende and garnet-vesuvianite zones), and a local marble zone enriched in violet vesuvianite crystals. Dark brown vesuvianites are the common variety in the studied area, while Cr^{3+} contents explain the violet vesuvianite variety, with diagnostic absorption features at ~680 and ~548 nm. The latter is successfully used for the generation of the violet vesuvianite spectral index for automating the recognition of potential gemological samples.

The proposed spectral indices could provide advances and new approaches to support the spectral characterization

of other skarn targets and deposits, complementing previous studies worldwide with a similar goal. It could include the application of these spectral indices or even modified indices-based versions in different exploratory data and scales, such as airborne/orbital images, ground-based imaging spectroscopy of fresh outcrops, or drill cores. In addition, some reservations are also presented using reflectance spectroscopy for this case study. Minerals such as wollastonite and scheelite do not show spectral responses in the visible-shortwave infrared range, but future complementary studies using the thermal infrared spectral range could be applied to assess the continuous use of other spectral technologies in skarn environments.

ACKNOWLEDGMENTS

This study was funded in part by the Coordenação de Aperfeiçoamento de Pessoal de Nível Superior (CAPES) — Brasil (finance code 001), with the scholarship to the first author. The authors thank the Post-Graduation Program in Geosciences of Universidade Federal de Pernambuco (UFPE), the Vale Institute of Technology for accessing the ASD-FieldSpec, and the Laboratory of Gemology (UFPE) for the facilities. The third author thanks the National Council for Scientific and Technological Development (CNPq) for his research grant (process number 309493/2020-0).

ARTICLE INFORMATION

Manuscript ID: 20220035. Received on: 5 MAY 2022. Approved on: 4 SEPT 2022.

How to cite this article: Silva L.A., Carrino T.A., Santos L.C.M.L., Correa Pabón R.E. 2022. Spectral characterization of the Umbuzeiro Doce skarn target (Brazil): insights for the exploration of a W-Mo-gemological vesuvianite system. *Brazilian Journal of Geology*, **52**(4):e20220035 https://doi.org/10.1590/2317-4889202220220035

L.A.S. wrote the first draft of the manuscript and prepared Figures 1 to 11 and Table 1. T.C. aided the reflectance spectroscopy and data integration stages, the methodological approach, and improved the manuscript through corrections and suggestions. L.S. aided field work and sample collection, contributed to the methodological approach, and revised the manuscript. R.C.P. provided the reflectance data, contributed to the methodological approach, and revised the manuscript.

Competing interest: the authors declare no competing interests.

REFERENCES

Almeida F.F.M., Hasui Y., Brito Neves B.B., Fuck R.A. 1981. Brazilian structural provinces: an introduction. *Earth-Science Reviews*, **17**(1-2):1-29. https://doi.org/10.1016/0012-8252(81)90003-9

Archanjo C.J., Viegas L.G.F., Hollanda M.H.B.M., Souza L.C., Liu D. 2013. Timing of the HT/LP transpression in the Neoproterozoic Seridó Belt (Borborema Province, Brazil): constraints from U-Pb (SHRIMP) geochronology and implications for the connections between NE Brazil and West Africa. *Gondwana Research*, **23**(2):701-714. https://doi.org/10.1016/j.gr.2012.05.005

Bedell R., Crósta A.P., Grunsky E. (Eds.). 2009. *Remote sensing and spectral geology*. Littleton: Society of Economic Geologists, 270 p.

Brito Neves B.B., Fuck R.A., Pimentel M.M. 2014. The Brasiliano collage in South America: a review. *Brazilian Journal of Geology*, **44**(3):493-518. https://doi.org/10.5327/Z2317-4889201400030010

Brito Neves B.B., Santos E.J., Van Schmus W.R. 2000. Tectonic history of the Borborema Province, Northeastern Brazil. *In*: Cordani U.G., Milani E.J., Thomaz Filho A., Campos D.A. (Eds.). *Tectonic Evolution of South America*. Rio de Janeiro, 31st International Geological Congress, p. 151-182.

Caxito F.A., Santos L.C.M.L., Ganade C.E., Bendaoud A., Fettous E., Bouyo M.H. 2020. Toward an integrated model of geological evolution for NE Brazil–NW Africa: The Borborema Province and its connections to the Trans-Saharan (Benino-Nigerian and Tuareg shields) and Central African orogens. Brazilian Journal of Geology, 50(2):1-38. https://doi.org/10.1590/2317-4889202020190122

Clark R.N. 1999. Spectroscopy of rocks and minerals, and principles of spectroscopy. *In*: Rencz A.N. (Ed.). *Manual of remote sensing*. Remote Sensing for the Earth Science. New York: John Wiley and Sons, v. 3, p. 3-58.

Clark R.N., King T.V.V., Klejwa M., Swayze G.A., Vergo N. 1990. High spectral resolution reflectance spectroscopy of minerals. *Journal of Geophysical Research*, **95**(B8):12653-12680. https://doi.org/10.1029/JB095iB08p12653

Clark R.N., Roush T.L. 1984. Reflectance spectroscopy: quantitative analysis techniques for remote sensing applications. *Journal of Geophysical Research*, **89**(B7):6329-6340. https://doi.org/10.1029/JB089iB07p06329

Cloutis E.A. 2002. Pyroxene reflectance spectra: minor absorption bands and effects of elemental substitutions. *Journal of Geophysical Research*, **107**(E6):5039. https://doi.org/10.1029/2001JE001590

Costa M.A.C., Perrotta M.M., Souza Filho C.R. 2017. Resultados preliminares de espectroscopia de refletância e imageamento hiperespectral na região da Mina de scheelita de Brejuí (RN), Faixa Seridó, Província Borborema. *In*: Simpósio Brasileiro de Sensoriamento Remoto. *Anais*... v. 18, p. 5737-5744.

Cudahy T.J., Wilson J., Hewson R., Linton P., Harris P., Sears M., Hackwell J.A. 2001. Mapping the skarn-porphyry-epithermal alteration system, at Yerington, Nevada, using VNIR-SWIR-TIR remotely sensed data. *Exploration and Mining Report*. 1121R.

Dantas E.L., Van Schums W.R., Hackspacher P.C., Fetter A.H., Brito Neves B.B., Cordani U., Nutman A.P., Williams I.S. 2004. The 3.4-3.5 Ga São José do Campestre massif, NE Brazil: remnants of the oldest crust in South America. *Precambrian Research*, **130**(1-4):113-137. https://doi.org/10.1016/j.precamres.2003.11.002

Ferreira A.C.M., Soares D.R., Lima R.J.S., Suassuna Filho J., Ferreira J.A.M. 2014. Vesuvianita violeta gemológica do skarn de Umbuzeiro Doce, Província Scheelitífera da Borborema, NE do Brasil. *Estudos Geológicos*, **24**(1):31-41. https://doi.org/10.18190/1980-8208/estudosgeologicos.v24n1p31-41

Fresia B., Ross P.S., Gloaguem E., Bourke A. 2017. Lithological discrimination based on statistical analysis of multi-sensor drill core logging data in the Matagami VMS district, Québec, Canada. *Ore Geology Reviews*, **80**:552-563. https://doi.org/10.1016/j.oregeorev.2016.07.019

Gaffey S.J. 1986. Spectral reflectance of-carbonate minerals in the visible and near infrared (0.35-2.55 microns): calcite, aragonite, and dolomite. *American Mineralogist*, **71**(1-2):151-162.

Groat L.A., Hawthorne F.C. 1998. Diffuse reflections and the symmetry of vesuvianite. *Phase Transitions*, **67**(1):137-151. https://doi.org/10.1080/01411599808219191

Groat L.A., Hawthorne F.C., Rossman G.R., Scott Ercit T. 1995. The infrared spectroscopy of vesuvianite in the OH region. *The Canadian Mineralogist*, **33**(3):609-626.

Guo N., Cudahy T., Juxing T., Qingxi T. 2019. Mapping white mica alteration associated with the Jiama porphyry-skarn Cu deposit, central Tibet using field SWIR spectrometry. *Ore Geology Reviews*, **108**:147-157. https://doi.org/10.1016/j.oregeorev.2017.07.027

Hecker C., Van Ruitenbeek F.J.A., Van der Werff H.M.A., Bakker W.H., Hewson R.D., Van der Meer F.D. 2019. Spectral absorption feature analysis for finding ore. A tutorial on using the method in geological remote sensing. *IEEE Geoscience and Remote Sensing Magazine*, **7**(2):51-71. https://doi.org/10.1109/MGRS.2019.2899193

Hollanda M.H.B.M., Archanjo C.J., Souza L.C., Armstrong R., Vasconcelos P.M. 2010. Cambriam mafic to felsic magmatism and its connections with transcurrent shear zones of the Borborema Province (NE Brazil): implications for late assembly of the West Gondwana. *Precambriam Research*, **178**(1-4):1-14. https://doi.org/10.1016/j.precamres.2009.12.004

Hollanda M.H.B.M., Souza Neto J.A., Archanjo A.J., Stein H., Maia A.C.S. 2017. Age of the granitic magmatism and the W-Mo mineralization in skarns of the Seridó belt (NE Brazil) based on zircon U-Pb (SHRIMP) and molybdenite Re-Os dating. *Journal of South American Earth Sciences*, **79**:1-11. https://doi.org/10.1016/j.jsames.2017.07.011

Hunt G.R. 1977. Spectral signatures of particulate minerals in the visible and near-infrared. *Geophysics*, **42**(3):501-513. https://doi.org/10.1190/1.1440721

Hunt G.R. 1979. Near infrared (1.3-2.4 μm) spectra of alteration minerals – Potential for use in remote sensing. *Geophysics*, **44**(12):1974-1986. https://doi.org/10.1190/1.1440951

Lampinen H.M., Laukamp C., Occhipinti S.A., Hardy L. 2019. Mineral footprints of the paleoproterozoic sediment-hosted Abra Pb-Zn-Cu-Au deposit Capricorn Orogen, Western Australia. *Ore Geology Reviews*, **104**:436-461. https://doi.org/10.1016/j.oregeorev.2018.11.004

Malvern Panalytical. 2022. ASD FieldSpec 4 Hi-Res NG Spectroradiometer. Available at: https://www.malvernpanalytical.com/en/products/product-range/asd-range/fieldspec-range/fieldspec-4-hi-res-ng-spectroradiometer. Accessed on: Apr. 22, 2022.

Medina C.M., Ducart D.F., Passos J.S., Oliveira L.R. 2021. Exploration vectoring from white mica spectral footprint in the atypical auriferous Lavra Velha deposit, San Francisco Craton, Brazil. *Ore Geology Reviews*, **139**(Part A):104438. https://doi.org/10.1016/j.oregeorev.2021.104438

Meinert L.D. 1992. Skarns and skarn deposits. *Geoscience Canada*, **19**(4):145-162.

Meinert L.D., Dipple M.G., Nicolescu S. 2005. World skarn deposits. *Economic Geology*, **100**:299-336. https://doi.org/10.5382/AV100.11

Mesquita N.M., Carrino T.A., Souza Neto J.A. 2019. The use of reflectance spectroscopy and the prehnite spectral index to target gold mineralization at the Bonfim polymetallic skarn deposit, Seridó Mobile Belt, Borborema Province, Brazil. *Ore Geology Reviews*, **115**:103192. https://doi.org/10.1016/j.oregeorev.2019.103192

Naleto J.L.C., Perrotta M.M., Costa F.G., Souza Filho C.R. 2019. Point and imaging spectroscopy investigations on the Pedra Branca orogenic gold deposit, Tróia Massif, Northeast Brazil: implications for mineral exploration in amphibolite metamorphic-grade terrains. *Ore Geology Reviews*, **107**:283-309. https://doi.org/10.1016/j.oregeorev.2019.02.019

Nascimento M.A.L., Galindo A.C., Medeiros V.C. 2015. Ediacaran to Cambrian magmatic suites in the Rio Grande do Norte domain, extreme Northeastern Borborema Province (NE of Brazil): Current knowledge. *Journal of South American Earth Sciences*, **58**:281-299. https://doi.org/10.1016/j.jsames.2014.09.008

Paixão M.S., Vieira F.F., Santos L.C.M.L., Silva F.M.R., Silva J.V., Lima M.G. 2019. Algumas considerações sobre a lente de skarn mineralizada em scheelita-vesuvianita de Umbuzeiro Doce, Paraíba. *In*: Simpósio de Geologia do Nordeste, 28., 2019, Aracaju. *Anais*... Aracaju: SBG, 2019. 1 p.

Pontual S., Merry N., Gamson P. 2008. *Spectral interpretation:* Field manual. GMEX. Spectral Analysis guides for mineral exploration. Victoria: AusSpec International Pty, 189 p.

Prado E.M.G., Silva A.M., Ducart D.F., Toledo C.L.B., Assis L.M. 2016. Reflectance spectroradiometry applied to a semi-quantitative analysis of the mineralogy of the N4ws deposit, Carajás Mineral Province, Pará, Brazil. *Ore Geology Reviews*, **78**:101-119. https://doi.org/10.1016/j.oregeorev.2016.03.007

Ross P.S., Bourke A., Schnitzler N., Conly A. 2019. Exploration vectors from near infrared spectrometry near the McLeaod Volcanogenic Massive Sulfide Deposit, Matagami District, Québec. *Economic Geology*, **114**(4):613-638. https://doi.org/10.5382/econgeo.4656

Santos E.J., Souza Neto J.A., Silva M.R.R., Beurlen H., Cavalcanti J.A.D., Silva M.G., Costa A.F., Santos L.C.M.L., Santos R.B. 2014. Metalogênese das porções norte e central da Província Borborema. *In:* Silva M.G., Rocha Neto M.B., Jost H., Kuyumjian R.M. (Eds.). *Metalogênese das províncias tectônicas brasileiras*. Belo Horizonte: CPRM, p. 343-384.

Santos F.G., Neto M.T.O.C., Ferreira V.P., Bertotti A.L. 2020. Eo to Paleoarchean metamafic-ultramafic rocks from the central portion of the Rio Grande do Norte Domain, Borborema Province, northeast Brazil: The oldest South American platform rocks. *Journal of South American Earth Sciences*, **97**:102410. https://doi.org/10.1016/j.jsames.2019.102410

Santos L.C.M.L., Caxito F.A. 2021. Accretionary models for the Neoproterozoic evolution of the Borborema Province: Advances and open questions. Brazilian Journal of Geology, 51(2):1-9. https://doi.org/10.1590/2317-4889202120200104

Souza Z.C., Kalsbeek F., Deng X.D., Frei R., Kokfelt T.F., Dantas E.L., Li J.W., Pimentel M.M., Galindo A.C. 2016. Generation of continental crust in northern part of the Borborema Province, northeastern Brazil, from Archean to Neoproterozoic. *Journal of South American Earth Sciences*, **68**:68-96. https://doi.org/10.1016/j.jsames.2015.10.006

Souza Neto J.A., Legrand J.M., Volfinger M., Pascal M.L., Sonnet P. 2008. W-Au skarns in the Neo-Proterozoic Seridó Mobile Belt, Borborema Province in northeastern Brazil: an overview with emphasis on the Bonfim deposit. *Mineralium Deposita*, **43**:185-205. https://doi.org/10.1007/s00126-007-0155-1

Tappert M., Rivard B., Giles D., Tappert R., Mauger A. 2011. Automated drill core logging using visible and near-infrared reflectance spectroscopy: a case study from the Olympic Dam IOCG deposit, South Australia. *Economic Geology*, **106**(2):289-296. https://doi.org/10.2113/econgeo.106.2.289

Tian J., Zhang Y., Cheng J.M., Sun S.Q., Zhao Y.J. 2019. Short wavelength infra-red (SWIR) characteristics of hydrothermal alteration minerals in skarn deposits: example from the Jiguanzui Cu-Au deposit, Eastern China. *Ore Geology Reviews*, **106**:134-149. https://doi.org/10.1016/j.oregeorev.2019.01.025

Van Schmus W.R., Brito Neves B., Hackspacher P.C., Babinski M. 1995. U/Pb and Sm/Nd geochronologic studies of the eastern Borborema Province, Northeastern Brazil: initial conclusions. *Journal of South American Sciences*, **8**(3-4):267-288. https://doi.org/10.1016/0895-9811(95)00013-6

Van Schmus W.R., Brito Neves B., Williams I.S., Hackspacher P.C., Fetter A.H., Dantas E.L., Babinski M. 2003. The Seridó Group of NE Brazil, a late Neoproterozoic pre- to syn-collisional basin in West Gondwana: insights from SHRIMP U-Pb detrital zircon ages and Sm-Nd crustal residence (T_{DM}) ages. *Precambrian Research*, **127**(4):287-327. https://doi.org/10.1016/S0301-9268(03)00197-9

Van Schmus W.R., Oliveira E.P., Silva Filho A.F., Toteu S.F., Penave J., Guimarães I.P. 2008. Proterozoic links between the Borborema Province, NE Brazil, and the Central African Fold Belt. *West Gondwana:* Pre-Cenozoic Correlations Across the South Atlantic Region. Geological Society Special Publication. London: The Geological Society, **294**:69-100. https://doi.org/10.1144/SP294.5

Velásquez Ruiz F., Giustina M.E.S.D., Oliveira C.G., Dantas E.L., Hollanda M.H.B. 2019. The 3.5 Ga São Tomé layered mafic-ultramafic intrusion, NE Brazil: Insights into a Paleoarchean Fe-Ti-V oxide mineralization and its reworking during West Gondwana assembly. *Precambrian Research*, **326**:462-478. https://doi.org/10.1016/j.precamres.2018.03.011

White A.J.R., Laukamp C., Stokes M.A., Legras M., Pejcic B. 2017. Vibrational spectroscopy of epidote, pumpellyite and prehnite applied to low-grade regional metabasites. *Geochemistry: Exploration, Environment, Analysis*, **17**(4):315-333. https://doi.org/10.1144/geochem2016-007

Yang H., Huntington J.F., Gemmell J.B., Scott K.M. 2011. Variations in composition and abundance of white mica in the hydrothermal alteration system at Hellyer, Tasmania, as revealed by infrared reflectance spectroscopy. *Journal of Geochemical Exploration*, **108**(2):143-156. https://doi.org/10.1016/j.gexplo.2011.01.001